Influence of mean pressure on aortic impedance and reflections in the systemic arterial system

JOE ALEXANDER, JR., DANIEL BURKHOFF, JOCHEN SCHIPKE, AND KIICHI SAGAWA
Department of Biomedical Engineering, The Johns Hopkins Medical School, Baltimore, Maryland 21205

ALEXANDER, JOE, JR., DANIEL BURKHOFF, JOCHEN SCHIPKE, AND KIICHI SAGAWA. *Influence of mean pressure on aortic impedance and reflections in the systemic arterial system.* Am. J. Physiol. 257 (Heart Circ. Physiol. 26): H969–H978, 1989.—The present investigation sought to determine the extent to which primary changes in mean arterial pressure (MAP) might influence the calculated aortic impedance. In seven open-chest, anesthetized, autonomically blocked dogs, we measured aortic impedance using white-noise analysis at various levels of MAP achieved by adjusting the height of a left atrial reservoir rather than by pharmacological intervention. Impedance spectra so obtained were parameterized according to best-fit windkessel models (R_a, R_c, C_a) and three parameters to characterize wave reflections: the frequency at which the phase of the impedance approached or crossed through 0° (ϕ_0), the frequency of the first minimum of the impedance modulus (f_{min}), and the amplitude of the first oscillation of the impedance modulus (a_1). The dependency of each of these parameters on MAP was investigated. In addition, we calculated the reflection coefficient spectrum (RCS). Results show that windkessel parameters were not significantly influenced by MAP and that the reflection parameters and the RCS depended on increased levels of MAP in a manner consistent with an increase in pulse-wave velocity.

white noise; aortic pressure; spectral analysis; global reflecting sites

AORTIC INPUT IMPEDANCE is frequently used to characterize the arterial afterload on ventricular ejection (6, 15, 18, 21). As is true for any proposed quantitative description of afterload, the impedance should ideally be independent of changes in heart rate and mean arterial pressure (MAP), both of which are variables that depend on ventricular function. Whereas aortic impedance has been shown to be independent of heart rate (9, 19), the influence of MAP has not been evaluated thoroughly, since previous studies relied on the use of pharmacological agents or efferent vagal stimulation (1, 10, 23), which, in addition to producing the intended effect of altering aortic input flow and pressure through ventricular effects, may also have incidentally altered arterial system properties.

The purpose of this investigation was to examine how the arterial impedance spectrum changes with primary changes in MAP. By "primary change" we emphasize the fact that MAP was varied by changing left ventricular filling pressure (and thus cardiac output) through use of a left atrial reservoir rather than by vagal stimulation or use of low-dose inotropic agents known to have secondary vascular effects. The response of the impedance to MAP changes was described in terms of changes in best-fit modified windkessel model parameters (30), as well as changes in several indexes of wave reflection. Because characterization of reflection phenomena relies sensitively on the ability to identify fine details of the impedance spectrum, i.e., impedance minima and maxima or zero crossings of phase, an emphasis was placed on determination of the impedance spectrum with a high resolution in frequency.

The white-noise approach to system identification has been described to be of particular utility in providing the type of high-resolution impedance spectra we needed to accurately assess the impedance minima and maxima that relate to arterial reflections (6, 10, 12, 28). Therefore, in a manner similar to that used by Taylor (28), we applied the approach to our investigation by making use of random pacing to increase the frequency content of aortic pressure and flow. Because the high-resolution spectra could be determined over a relatively short sampling interval, we performed repeated measures for calculation of coherence, a kind of frequency-domain correlation function between aortic pressure and flow, which, if low, would serve as an index of nonlinear or time-varying vascular system behavior.

MATERIALS AND METHODS

Surgical and measurement procedures. Data were obtained from a total of seven mongrel dogs of either sex, weighing 23 ± 3.1 (SD) kg. Each dog was anesthetized with pentobarbital sodium (30 mg/kg iv), intubated, and respired on room air supplemented with 95% O_2-5% CO_2 at a rate of 4–5 l/min. The thorax was opened via a median sternotomy in addition to a left lateral thoracotomy in the fourth intercostal space; the latter was performed to allow easy access to the left atrium (to which a reservoir was connected, as described below). The proximal aortic root was exposed by blunt dissection of the surrounding adipose and connective tissue. A Transonic flow probe of either 16 or 20 mm diam was positioned around the aortic root as close to the aortic valve outlet as possible for measurement of aortic flow. The flowmeter (Transonic Systems, Ithaca, NY), using the principle of ultrasonic transit time, measured volume flow directly, irrespective of vessel size and flow velocity profile, and provided automatic zeroing and calibration capabilities. Acoustic coupling between the aorta and flow probe was maintained by commercially available jelly. With such a flow measurement system, the probe

diameter could be chosen to be larger than that of the vessel, eliminating any concern over constriction of the aorta causing secondary alterations in local mechanical properties. The flowmeter introduced a fixed 8-ms delay that was corrected for in calculations of the impedance spectra. To measure aortic pressure at the site of the flow probe, a 7-Fr micromanometer-tipped Millar catheter was introduced into the left femoral artery and advanced to a position just distal to the flow probe, as indicated in Fig. 1 and described as follows. With the catheter sitting within its core, the flow probe fails to operate properly because of acoustic interference, and this is manifest by noise on the flow signal and loss of the zero base line. Making use of this fact, we initially advanced the catheter into the left ventricle then slowly withdrew it, first until it came within the field of the flow probe, then a bit more until a clean signal was obtained with normal zero during diastole. Proper catheter positioning by this method was confirmed at the end of several experiments by direct inspection after dissection of the aortic wall. For monitoring of the left ventricular pressure, a 7-Fr micromanometer-tipped Millar catheter was inserted into the left ventricle through an apical stab incision.

The left atrium was cannulated with a line connected to a blood reservoir, the height of which could be adjusted by a pulley mechanism. Changing the height of the reservoir altered the filling pressure of the left ventricle, thus providing a way of controlling MAP. A unipolar pacing lead was sutured to the left ventricular free wall, as were two additional leads for measuring a bipolar surface electrocardiogram. The right and left common carotid arteries were isolated so that they could be clamped intermittently during the experiment to assess the status of hexamethonium-induced baroreceptor reflex blockade.

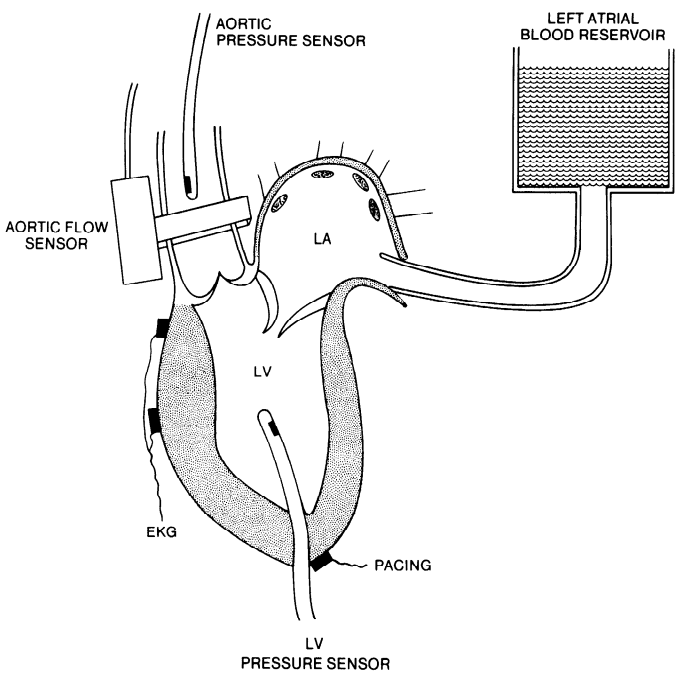

FIG. 1. Biological preparation. Instrumented left heart and aorta are shown. Mean pressure was varied by adjusting height of a blood reservoir connected to the left atrium (LA) via a cannula. Millar pressure sensors were placed inside left ventricle (LV) as well as in aorta. Aortic pressure was measured just distal to ultrasonic aortic flow sensor as shown. Heart was paced from LV free wall. A surface electrocardiogram (EKG) was monitored.

Experimental protocol. To obtain canine aortic input impedance spectra under a wide variety of MAPs but constant arterial state, we first blocked baroreceptor reflexes with a bolus injection of hexamethonium (15 mg/kg iv). Blockade was checked hourly by examining the response in blood pressure to 30-s bilateral common carotid occlusion; if a response was noted, an additional 5 mg/kg was administered and the procedure repeated until there was no response. Vasodilation and consequent fall in arterial pressure occurred rapidly with the administration of hexamethonium, making it necessary to start continuous infusion of phenylephrine (40–100 μg/min) or epinephrine (5–10 μg/min) intravenously to maintain a constant vascular tone while keeping the MAP within the normal range (100–130 mmHg) for a normal left ventricular end-diastolic pressure. When the response to continuous drug infusion reached a steady state, data acquisition was initiated.

Three sets of aortic pressure and flow data were acquired at each level of MAP: before random stimulation, with the heart beating at a constant rate; during random stimulation; and after cessation of random stimulation, with the heart beating again at a constant rate. The rationale behind measuring the first and third sets of periodic pressure and flow data (the control and recontrol data for the random sequence) was twofold: *1*) to provide a simple mathematical check of whether the impedance calculated from the more complex "aperiodic" random sequence was in agreement with that calculated from the control "periodic" signal at frequencies they had in common, i.e., at harmonics of the fundamental frequency, and *2*) to provide a check of the stability of the preparation over the course of the random sequence. All three sets of data were in tight agreement at harmonics of the fundamental frequency in all animals studied.

Random pacing in these experiments was accomplished through the use of a digitally controlled pacer, receiving its trigger command signal from a computer. The trigger signal was composed of a uniform random sequence of zeros and ones in which a single value from the sequence would be sent out to the pacer every 200 ms. When the pacer would receive a low value (0), it remained silent as if no trigger was received at all; a high value (1) would trigger the pacer, causing it to stimulate the ventricle. The minimum possible interval of 200 ms between successive stimuli was chosen to fall roughly outside the refractory period of the cardiac action potential.

From each animal we were usually able to obtain spectra at four or five distinct levels of MAP, spanning an overall range of 120 mmHg, from as low as 50 to as high as 170 mmHg. MAP was varied by changing the height of the left atrial reservoir not by changing the rate of vasoconstrictor infusion. It is important to acknowledge that although we could control MAP for each random protocol, we had no control over the pressure distribution about each of the means. Typically, the distribution of pressures was skewed slightly in the di-

rection of higher pressures and broadened as mean pressure was increased. Figure 2 shows example aortic pressure distributions obtained during random protocols at disparate mean pressures. If the system is only quasi-linear and the distribution of pressures during a random protocol is broad enough, we might experience considerable variability within a given run because of system nonlinearities. The poor quality of such data would be reflected in our coherence calculation.

The order in which MAP was varied within a given experiment was also randomized to minimize the effects of any systematic error or slow vascular adaptation that might come from always changing MAP in a particular sequence.

Determination of impedance and coherence. Aortic input impedance was calculated from the digitized aortic pressure and flow signals obtained during random ventricular pacing. The use of random stimulation, or so-called "white noise," to determine the characteristics of biological systems is reviewed in detail by Marmarelis and Marmarelis (12). Our particular methods for determining the impedance and coherence functions have been described previously in detail (6).

We emphasize that the measurement of coherence is important to our study, since, by the very nature of our analysis, i.e., the use of the Fast Fourier Transform (FFT), we tacitly assume at least quasi-linear behavior of the arterial system, i.e., we assume linear system behavior of the input-output relationship around a given MAP. The coherence serves as a measure of the validity of that assumption. If the coherence is poor, not only is the assumption invalidated, but the whole analysis is invalidated on mathematical grounds; if the coherence is good, the quasi-linear assumption is valid, and our use of Fourier Analysis in this application is appropriate.

Determination of best-fit windkessel parameters. The three parameters of the windkessel model that best fit each measured spectrum were obtained as follows. The characteristic impedance (R_c) was set equal to the arithmetic mean of the magnitude of the impedance spectrum >2 Hz as proposed previously by other investigators (2, 6, 16, 25). The peripheral arterial resistance (R_a) was taken as the difference between the measured direct current resistance (i.e., the modulus of the impedance at 0 Hz) and R_c. To estimate the arterial compliance (C_a), we used a method outlined recently by Liu (11) and applied to pseudorandom pressure data by Burkhoff et al. (6).

Identification of reflection parameters. As a means of roughly quantifying arterial reflections, we have identified three parameters from the high-resolution impedance spectra. They are ϕ_0, the frequency at which the phase of the impedance sharply approaches or crosses through zero degrees; f_{min}, the frequency of the first minimum of the impedance modulus; and a_1, the amplitude of the first oscillation of the impedance modulus. These parameters were chosen because they relate to changes in the arterial impedance spectrum known to accompany changes in pulse-wave velocity and the magnitude of reflected waves (10, 21, 23).

RESULTS

Figure 3 shows a recording of a typical set of pressure and flow tracings obtained during random left ventricular stimulation. The MAP during this particular random run was ~140 mmHg. Note the stability of the zero base line of flow during diastolic pressure decay, despite the irregular ventricular rate. This stability was maintained even during random pacing at MAPs as low as 50 mmHg. There are two reasons for this: one is that unlike for the case of electromagnetic flow measurement, the electrocardiogram does not manifest itself as noise in the flow signal, and the other is that the vessel is not required to always stay in contact with the flow probe as long as acoustic coupling is maintained. Thus, even during the long diastoles that invariably occurred in our random

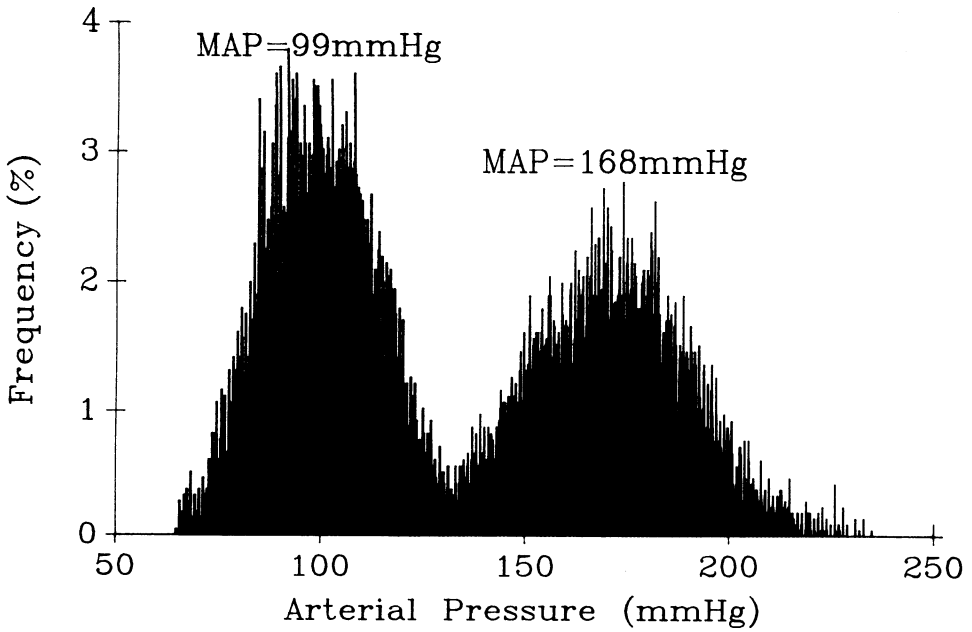

FIG. 2. Histograms showing frequency distributions of pressures about mean values during 2 different random pacing protocols. Note broadening of distribution at higher mean arterial pressure (MAP).

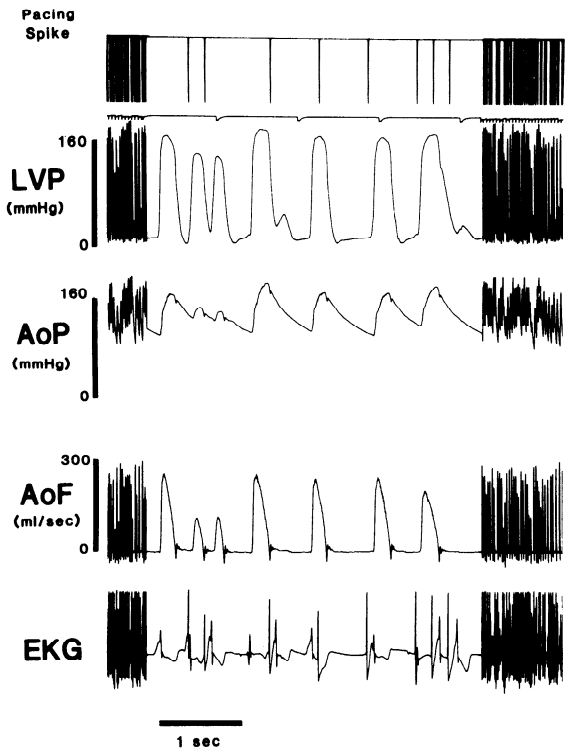

FIG. 3. Typical pressure and flow tracings obtained during random pacing at a constant mean pressure of ~140 mmHg. From *top* to *bottom* are tracings of pacing spike, left ventricular pressure (LVP), aortic pressure (AoP), aortic flow (AoF), and bipolar surface electrocardiogram (EKG).

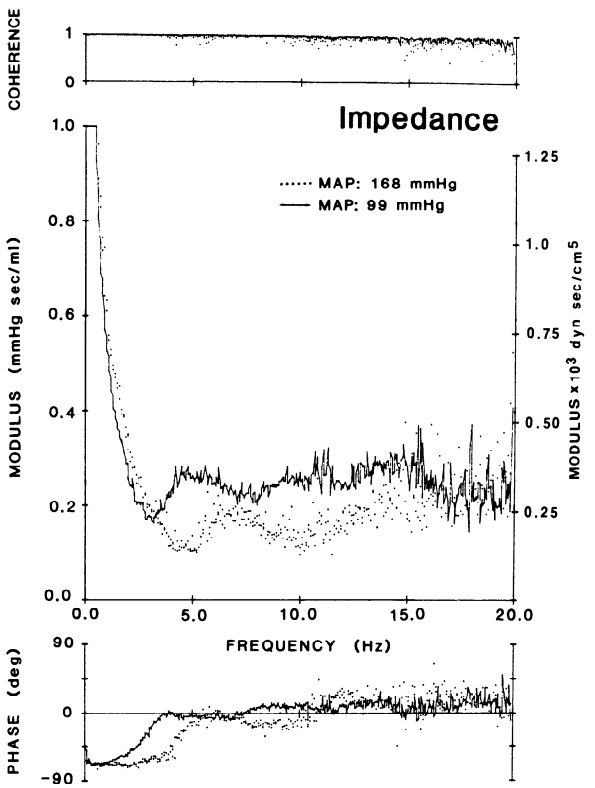

FIG. 4. Superimposed impedance spectra determined at 2 disparate mean arterial pressures (MAP). Coherences, impedance moduli, and phase spectra obtained at MAP of 99 and 168 mmHg are shown. At either MAP, coherences were quite close to unity across a broad frequency band. Increasing MAP caused a rightward shift of modulus (and phase), resulting in higher amplitudes in low-frequency range (<~3 Hz) and diminished amplitudes across higher frequencies. Direct current resistance for spectrum obtained at 99 mmHg is 11.9 mmHg·s/ml; that obtained at 168 mmHg is 13.4 mmHg·s/ml.

pacing protocols, in which the aortic pressure was apt to drop to levels that allowed the vessel to shrink away from the flow probe, the flow signal remained stable as long as an acoustic couplant (ultrasonic jelly, coagulated blood, etc.) was liberally applied.

Also, note from Fig. 3 that ejecting contractions deriving both from random external stimulation and ventricular ectopic beats contributed to arterial system flow input.

Effect of MAP on windkessel parameters. The effect of two levels of MAP on the broad-band high-resolution impedance spectrum is exemplified in Fig. 4. Each spectrum is expressed as an impedance modulus (*center*) and phase (*bottom*). The coherences at all frequencies of each spectrum are also plotted (*top*). Note that in each case the coherence remains very close to unity across all frequencies, indicating linear behavior of the system about each MAP throughout the course of the measurements. It should also be noted that (aside from windowing) the impedance spectrum is not smoothed; each point represents an actual measurement.

R_c is the windkessel parameter most obviously affected in the example of Fig. 4. Increasing MAP from 99 to 168 mmHg caused a slight decrease in R_c from 0.25 to 0.19 mmHg·s/ml, an increase in R_a from 11.6 to 13.2 mmHg·s/ml, and a drop in C_a from 0.29 to 0.25 ml/mmHg. (Note that the scaling of the impedance modulus plot was set to provide adequate resolution of the spectrum at higher frequencies and that the very low frequency points are not displayed.)

Data from all seven dogs showing the effect of MAP on best-fit windkessel parameters are shown in Fig. 5. In all animals but one, R_c showed a consistent (although not statistically significant) decline with increasing MAP. The value of R_c is thought predominantly to reveal the local mechanical characteristic impedance of large arteries close to the specific recording site (27, 29). Because the R_c of arterial segments depends primarily on mechanical and geometric properties (4), and because these properties are known to be sensitive to mean pressure owing to nonuniformity of elastic properties of arteries (5), our finding of a relatively constant R_c from the vascular impedance spectrum was somewhat surprising. Nevertheless, our results are corroborated by previous investigators who also found a slight but not statistically significant decrease in R_c with increasing MAP (7, 23). The other windkessel parameters, R_a and C_a, showed no clear association to MAP changes in the range studied.

Effect of MAP on reflection parameters. In general, changes in MAP had a significant effect on our reflection parameters, which is very apparent in Fig. 4. The example shows that increasing MAP caused a shift in ϕ_0 from 3.6 to 5.6 Hz, a shift in f_{min} from 3.2 to 5.1 Hz, and a reduction in a_1 from 0.27 to 0.18 mmHg·s/ml. The reflection data obtained at multiple MAPs in each of the seven dogs is shown in Fig. 6. Note that in contrast to

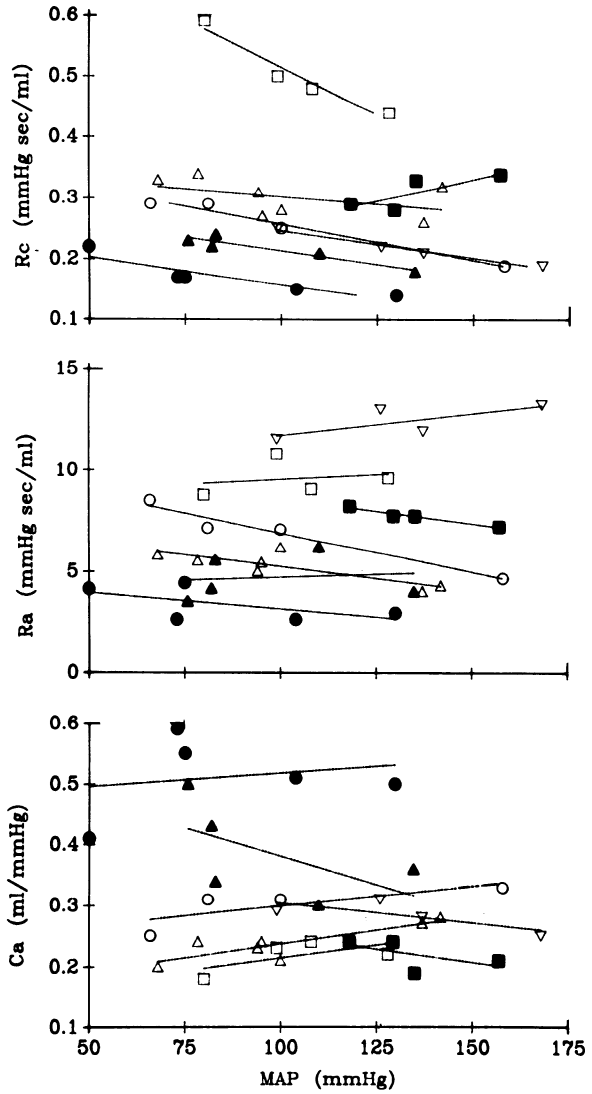

FIG. 5. Summary of results from individual dogs (n = 7) showing effect of mean arterial pressure (MAP) on best-fit windkessel parameters. Symbol types are unique to a given dog, and regression lines are superimposed. R_c, characteristic impedance; R_a, peripheral arterial resistance; C_a, arterial compliance.

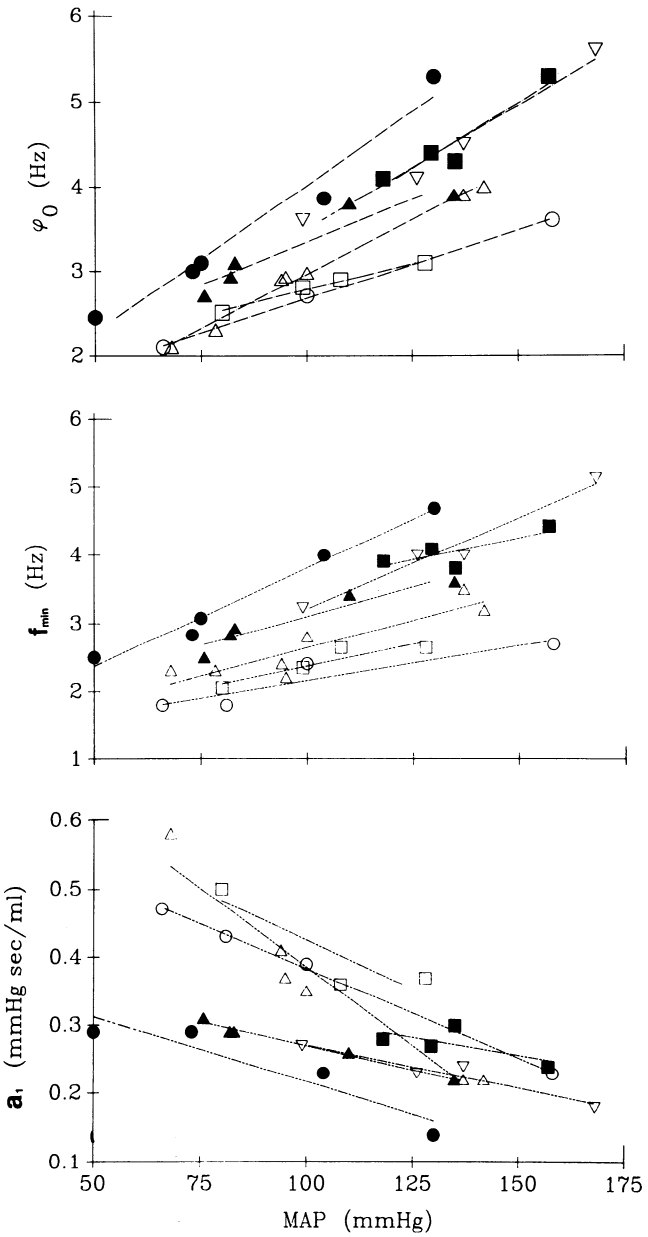

FIG. 6. Plots showing influence of mean arterial pressure (MAP) on reflection parameters. In contrast to windkessel parameters, these showed a consistent and significant dependency on MAP. ϕ_0, frequency at which phase of impedance approaches or crosses 0°; f_{min}, frequency of 1st minimum of impedance modulus; a_1, amplitude of 1st oscillation of impedance modulus.

the relative lack of dependency of the windkessel parameters on MAP, the reflection parameters show a consistent and significant dependency. ϕ_0 and f_{min} increase for all animals with increases in MAP, whereas a_1 decreases.

For each of the six parameters (windkessel and reflection parameters) plotted as functions of MAP, regression lines from individual animals were examined. For a given parameter, the slopes of the seven regression lines were compared with slopes of zero, using a two-sided paired t statistic to test the hypothesis that the measured slopes were not different from zero. (A slope of zero is what should be expected of a purely linear system in which parameters should be independent of the level of the input, i.e., of MAP.) The statistical test was applied to the data from all seven dogs for each parameter assuming a 5% significance level. The results indicate that systemic arterial reflections are significantly affected by primary changes in MAP, although windkessel parameters are not affected.

Reflection coefficient spectrum and its dependency on MAP. Characterization of arterial wave reflection phenomena by impedance-derived parameters (ϕ_0, f_{min}, and a_1) is convenient but somewhat limited. Because impedance expresses the relationship between pressure and flow, rather than between the incident and reflected components of either pressure or flow, parameters derived from the impedance spectrum do not provide a direct representation of reflection. Therefore, as a further more explicit characterization of the effect of MAP on reflections, we calculated the reflection coefficient spectrum (RCS), defined as the frequency-dependent ratio of reflected to forward pressure (or flow) waves.

To calculate RCS, we assumed the systemic arterial bed to behave as if it were a lossless transmission line of

a certain R_c terminated by a load impedance [$(Z(\omega)$], which is the arterial impedance (10, 17, 32). The governing equation is the simple relation

$$\Gamma(\omega) = \frac{Z(\omega) - R_c}{Z(\omega) + R_c}$$

where $\Gamma(\omega)$ is the frequency-dependent RCS. The example shown in Fig. 7 is calculated using the impedance spectra of Fig. 4 and shows features that are representative of all the RCS spectra determined from our study; namely, that with elevation of MAP there was *1*) an increase in the RCS modulus and *2*) an accompanying rightward shift of the RCS phase toward higher frequencies. The rightward shift in phase with an increase in MAP is consistent with reduction of the transit time of a wave traveling between the recording site and global arterial reflecting sites. The decreased transit time is due to increased pulse-wave velocity (8, 23).

DISCUSSION

We employed high-resolution impedance analysis to determine the influence of MAP on arterial system properties. Previous investigators who changed MAP to explore the linearity of the arterial impedance did so by infusing low-dose pharmacological agents or by applying efferent vagal stimulation presumed to act primarily on the heart (9, 19, 23). However, such interventions may have changed MAP not only by altering cardiac output but also by potentially changing the properties of the very system that was to be characterized. We circumvented these undesirable secondary effects by measuring impedance at a constant vascular tone, with MAP changes achieved by changing the height of a left atrial reservoir. Furthermore, the white-noise approach enabled us to resolve impedance minima, maxima, and zero crossings of phase with a much better frequency resolution than used in previous studies that examined the influence of MAP on the hydraulic input impedance. We also calculated the coherence, an index of mathematical certainty in the measured impedance data.

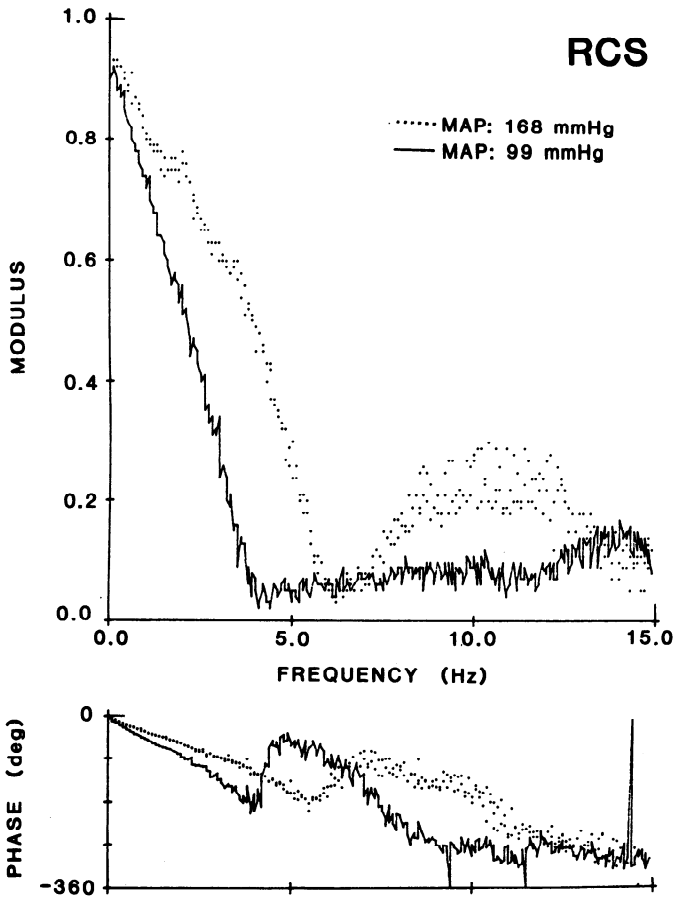

FIG. 7. Superimposed reflection coefficient spectra measured at disparate mean arterial pressures (MAP). Shown are amplitude and phase spectra obtained at MAP of 99 (——) and 168 mmHg (· · · · ·). These reflection spectra were calculated from impedance spectra of Fig. 4. Increasing MAP caused a distinct increase in reflection coefficients as well as a notable rightward shift in phase across virtually the entire frequency range. RCS, reflection coefficient spectrum.

One part of our analysis indicated that the arterial system, expressed in terms of best-fit windkessel parameters, is linear over a fairly broad range of mean pressures; that is, there was no statistically significant influence of MAP on R_c, R_a, or C_a. The finding of a relatively constant R_c from the vascular impedance spectrum over a broad range of MAPs was surprising in light of the reported nonuniformity of elastic properties of arteries (5) and the fact that our reflection indexes showed evidence of an increase in pulse-wave velocity. However, other investigators have documented these same findings (7, 8, 23). To elucidate this apparent discrepancy of findings, Cox (8) performed a series of experiments wherein he simultaneously measured intra-arterial pressure and aortic external diameter at multiple sites and computed values of wall geometry, dynamic modulus, phase velocity, and local mechanical characteristic impedance. Interestingly, he found that whereas dynamic elastic modulus and phase velocity increased with mean pressure at each arterial site, values of computed characteristic impedance were constant and independent of mean arterial pressure between 80 and 150 mmHg. The data presented by Cox (8) also showed that as mean pressure was increased, inner and outer diameters of most arterial segments also increased. Such an increase in diameter would counterbalance the increase in phase velocity, tending to produce a constant characteristic impedance. This study by Cox (8) of local mechanical arterial properties provides direct support for our vascular characteristic impedance results, indicating that the pressure dependency of mechanical and geometric arterial wall properties are such that they produce an essentially constant characteristic impedance with changes in MAP. Regarding the other windkessel parameters (R_a and C_a), we could not find results in the literature against which to compare ours, since to the best of our knowledge, the influence of MAP on R_a and C_a determined from the vascular input impedance has not been investigated previously.

Results similar to ours on the more general characteristics of arterial impedance spectra measured at various blood pressure levels in anesthetized animals have been reported (1, 9, 10, 23, 24). O'Rourke and Taylor (23) found that blood pressure changes arising from varying degrees of cardiac efferent nerve stimulation affected

aortic impedance amplitude spectra essentially by shifting them to the left when blood pressure decreased and to the right when it increased. Abel (1) found that amplitude spectra increased when blood pressure was changed by vasoconstriction (phenylephrine and norepinephrine) and decreased with vasodilatation (isoproterenol). In the present study in which primary changes in blood pressure were brought about through the use of a left atrial reservoir mechanism, we observed the responses of previous investigators just outlined (see Fig. 4 as an example): *1*) increased blood pressure resulted in rightward shifts of impedance modulus and phase, and *2*) increased blood pressure resulted in an increased amplitude spectrum in the low-frequency range, although typically a somewhat diminished amplitude spectrum at higher frequencies resulting in a slight decrease in R_c. These findings in our preparation indicate that pure changes in blood pressure alone are sufficient to cause the changes in impedance spectra noted previously in response to neurohumoral interventions that may have changed vascular tone in addition to changing blood pressure (1, 10). Latson (10), who investigated the effect of nitroglycerin on the impedance spectrum, obtained results very similar to those we obtained in response to decreased blood pressure, although in his preparation blood pressure was controlled.

In contrast to our results on windkessel parameters, the three reflection parameters were significantly influenced by changes in blood pressure. ϕ_0 and f_{min} increased with increasing blood pressure, indicating an increase in pulse-wave velocity. However, the change in a_1 is counterintuitive. If, as the other indexes indicate, reflections are noted to increase with increasing blood pressure, then, by intuition, the terminating load impedance causing the reflections should be increased as well. To the contrary, a_1 is consistently found to decrease with increasing blood pressure. We interpret this apparent contradiction as having to do with the rightward shift in the spectrum in the case of increased blood pressure. We postulate that because reflection phenomena in the arterial system are low-pass filtered, a rightward shift of the impedance amplitude spectrum would subject a_1 to a greater degree of attenuation. This hypothesis is supported by the fact that in the low-frequency range (<3–5 Hz) the amplitude spectrum is indeed higher at higher blood pressures. Attenuation of higher frequency components of the rightward-shifting amplitude spectrum might also explain why the estimated R_c tends to slightly decrease with increasing blood pressure.

We calculated the global reflection coefficient spectrum to examine whether it might provide clearer insight into the effect of blood pressure on reflections. The amplitude (but not the phase) of this spectrum has been presented by earlier investigators as a means of describing arterial reflections (10, 32). The transformation from the impedance spectrum to the RCS is mathematically very simple (see *Eq. A1* in the APPENDIX). Because the latter representation directly shows the relationship between forward and reflected pressure (or flow) wave components, it may substantially improve intuitive understanding of reflection phenomena (compare Figs. 4 and 7, which were calculated from the same data, for an example). Even in the high-gain plot of Fig. 4, the increase in the impedance amplitude in the lower frequency accompanying increased blood pressure appears unimpressive; moreover, as discussed above, the impedance amplitudes actually drop below control levels at higher frequencies. On the other hand, the global RCS of Fig. 7 shows a clear increase in the magnitude of reflections and a distinctly rightward shift in phase over virtually the entire frequency range.

Regarding the shape of the reflection coefficient amplitude spectrum, there is obvious damping of reflected waves at higher frequencies at any mean pressure. This low-pass filtering has been reported by past investigators (10, 29, 32) and is presumed to be due to a combination of the following: *1*) elastic and geometric differences, such as tapering, between proximal and distal portions of the arterial tree, *2*) damping by viscous effects during wave transmission, and *3*) frequency-dependent damping at the effective terminal reflecting sites. Part of the decrease in the reflection coefficient amplitude may be due not to damping but to reflected waves returning from the periphery with random phases, since the lengths traveled are considerable with respect to their wavelengths (29, 31).

The phase characteristics of the global RCS, which have been ignored previously, are also very informative. Consider the spectrum in the top left panel of Fig. 8. Shown are the amplitude and corresponding phase spectra obtained at a constant mean pressure. Arbitrarily, 360° was added to the phase angle if it passed through −360° so that phase would not exceed the −360° plotter window. Notice in this example how the phase accelerates as it approaches −360° at ~5 Hz. This sharp inflection of phase in the vicinity of 5 Hz (as it tends toward −360°) is a rather characteristic feature of the RCS phase spectrum and is determined by the interaction of upper and lower body reflected waves (discussed below). The frequency at which the phase would cross through −360° is of special importance; it is directly related to the transit time required for a wave to travel from the pressure and flow recording site in the aorta out to some global arterial reflecting site and back. In fact, if the arterial system were modeled as a single tube terminated by a load impedance and having no damping of the reflection coefficients, the frequency at which the phase would cross through −360° would exactly equal the reciprocal of the transit time ($1/T_d$). In such a model, the phase would circumvolve the unit circle ad infinitum (passing through integer multiples of −360°), with each revolution requiring a time of T_d to complete.

The steep inflection in the RCS phase can be explained by a model that assumes the existence of a second tube in parallel and out of phase with the first. Many investigators have reported on the lack of validity in assuming the arterial system to behave in the intact situation like a single tube and have proposed various multibranched models for the structure of the arterial tree (3, 10, 14, 20, 22, 26, 29, 31, 32). To facilitate an understanding of the modulus and phase characteristics of the measured RCS, we considered the behavior of an asymmetric T (two-

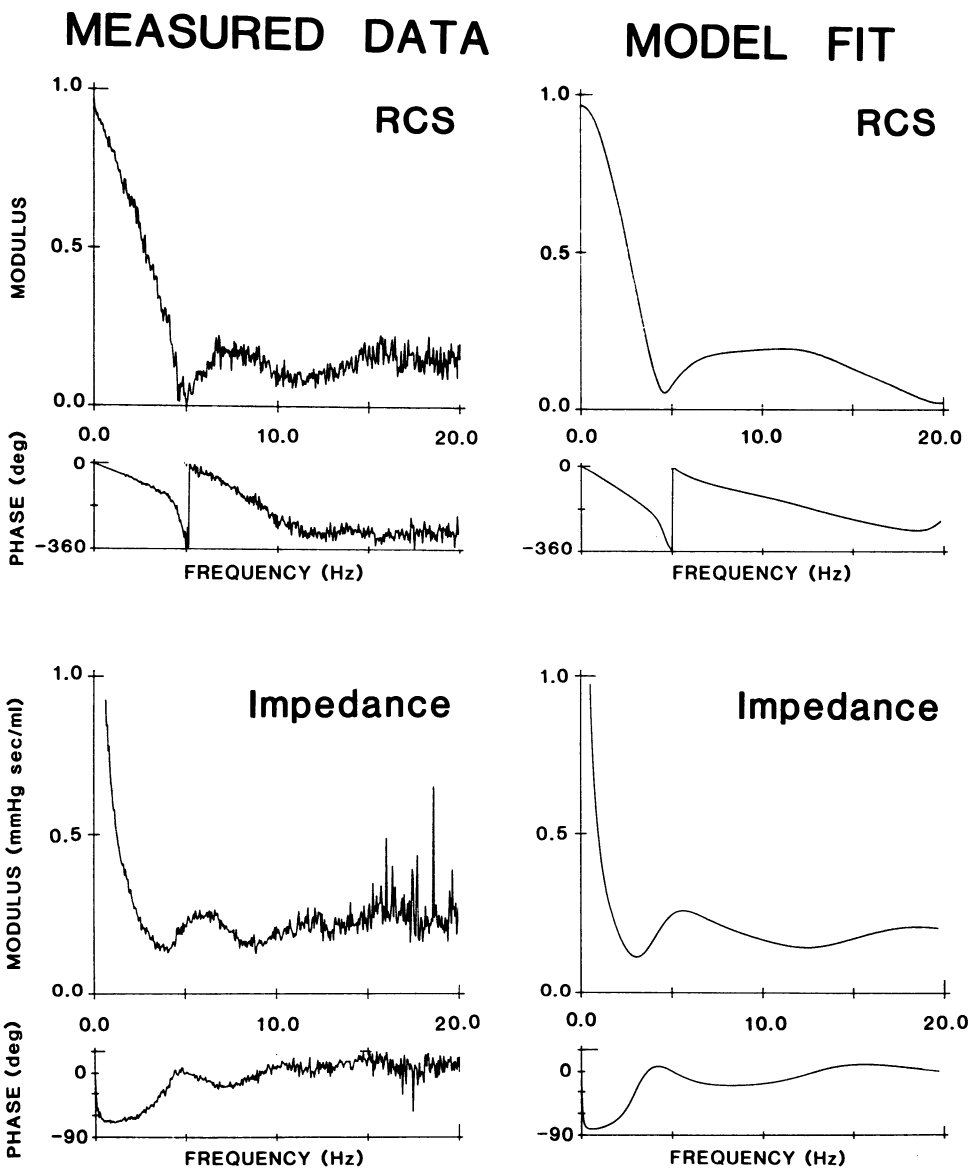

FIG. 8. Model fit of a reflection coefficient spectrum (RCS) and its corresponding impedance by empirical adjustment of only 4 parameters in a two-tube (asymmetric T) model, with damping of reflection coefficients. Fit is not exact, but notice model representation of even some of the more subtle features of RCS phase, such as its sudden acceleration toward −360° at 5 Hz.

tube) model of the arterial system, the combination of an upper and lower body tube of different lengths arranged in parallel, with damping of reflection coefficients for each tube. Such a model captures the essential features of observed impedance and RCS on empirical adjustment of only four parameters, the transit times (T_d) and corner frequencies for low-pass filtering of reflection coefficients (ω_c) for the upper and lower body tubes. It was not necessary to empirically adjust direct current and R_c parameters, since they were easily obtained from the experimentally determined impedance spectrum. The details of the model are explained in the APPENDIX.

The top right panel of Fig. 8 shows the result of empirical parameter adjustment for fitting the reflection data. This fit was obtained by using for the lower and upper body tubes, respectively, corner frequencies of 2 and 3 Hz and transit times of 0.1 and 0.02 s. We were able to identify what would be reasonable estimates of transit times based on a previous study by McDonald (13) in which he reported measurements of regional arterial pulse-wave velocity. Furthermore, by inspecting the shape of the measured spectrum, we guessed that the corner frequencies for damping of each of the two tubes would both be <5 Hz. Finally, we anticipated that reflections in the upper tube would be less attenuated (i.e., have a higher corner frequency) than those occurring in the lower tube. We were surprised by the remarkable agreement in both modulus and phase between the measured and computed reflection spectra.

With the assumption that this model is valid, interpretation of the characteristics of the measured global reflection coefficient spectrum becomes a simple matter. The low-frequency range is dominated by the longer, lower body tube and the high-frequency range by the upper body tube which is shorter. These tubes are not only of different lengths, but they may each filter reflections to different degrees (owing to geometric differences). The RCS can be remarkably well represented as the sum of two vectors in the complex plane, one vector for each tube. The dip in the reflection coefficient phase spectrum (occurring at ~4 Hz in Fig. 7 and 5 Hz in Fig. 8) signifies the frequency of transition above which the

upper tube becomes the predominant component of the vector sum in determining the net magnitude of reflections and transit times of the combined tubes. Therefore, the change in the reflection phase spectrum noted in Fig. 7 in response to increasing blood pressure may be due not only to an increase in pulse-wave velocity seen in both tubes but also an increase in the relative contribution of the lower body tube compared with the upper body tube in determining reflections at higher frequencies (i.e., rightward shift of the dip frequency).

Finally, without altering the model parameters chosen to fit the RCS of Fig. 8, we compared the impedance spectra corresponding with both the measured (*left*) and modeled (*right*) reflection spectra. They too were remarkably similar.

In summary, we found the arterial hydraulic impedance to be linear in its windkessel parameters over a fairly broad range of mean pressures. However, reflection parameters showed a significant dependency on mean pressure. The changes in the impedance spectra we observed in response to primary decreases in MAP were similar to those reported previously by Latson (10), who controlled MAP and administered a vasodilator (nitroglycerin) to change arterial reflections. This implies that under ordinary conditions vasoactive substances may alter reflections by way of two additive mechanisms, a change in blood pressure per se and a change in vascular tone. We also found that the pressure dependency of one of the parameters, a_1, appeared to be somewhat counterintuitive until we examined the RCS with scrutiny. We found that by considering a two-tube model of the arterial system, in which the upper and lower body tubes might damp reflected waves differently, we could evaluate the measured RCS with intuitive satisfaction. Evaluating reflections in the latter domain, we could escape some of the apparent ambiguities that might often result from using an impedance representation to make inferences about reflections. Moreover, we believe the phase information of the RCS to be at least as informative as the amplitude spectrum in understanding reflections.

APPENDIX

Two-Tube Model of Systemic Arterial Load with Low-Pass Filtering of Reflected Waves

The terminating load impedance for a single-tube model of the systemic arterial system, assuming lossless transmission line characteristics, can be described by the following equation

$$Z(\omega) = R_c\left[\frac{1 + \Gamma(\omega)}{1 - \Gamma(\omega)}\right] \qquad (A1)$$

where

$$\Gamma(\omega) = \omega_c/(j\omega + \omega_c)\Gamma_0 e^{-(j\omega T_d)} \qquad (A2)$$

for the case in which the transmission time, T_d, is not negligible, and the reflection coefficients are low-pass filtered at a corner frequency of ω_c (expressed in radians) and where $j\omega$ is an imaginary number. Substituting this expression for $\Gamma(\omega)$ into *Eq. A1* yields

$$Z(\omega) = R_c\left[\frac{1 + \omega_c/(j\omega + \omega_c)\Gamma_0 e^{-j(\omega T_d)}}{1 - \omega_c/(j\omega + \omega_c)\Gamma_0 e^{-j(\omega T_d)}}\right] \qquad (A3)$$

Substituting the relation

$$e^{-(j\omega T_d)} = \cos(\omega T_d) - j\sin(\omega T_d) \qquad (A4)$$

into *Eq. A3* and simplifying produces *Eq. A5*

$$Z(\omega) = R_c\left\{\frac{\omega_c[1 + \Gamma_0\cos(\omega T_d)] + j[\omega - \omega_c\Gamma_0\sin(\omega T_d)]}{\omega_c[1 - \Gamma_0\cos(\omega T_d)] + j[\omega + \omega_c\Gamma_0\sin(\omega T_d)]}\right\} \qquad (A5)$$

The four input parameters necessary to solve *Eq. A5* are ω_c, T_d, R_c, and R_{DC}. [Γ_0 can be readily derived from the relation $\Gamma_0 = (R_{DC} - R_c)/(R_{DC} + R_c)$ once parameters R_{DC} and R_c are specified.]

In the case of the asymmetric T model of the arterial system (i.e., 2 tubes of differing characteristics arranged in parallel), *Eq. A5* may be written independently for the upper (up) and lower (lo) body tubes and combined in parallel to yield the total load impedance [$Z_t(\omega)$]

$$Z_t(\omega) = \frac{Z_{up}(\omega)Z_{lo}(\omega)}{Z_{up}(\omega) + Z_{lo}(\omega)} \qquad (A6)$$

The RCS for the combined system may then be simply calculated using *Eq. A7*

$$\Gamma_t(\omega) = \frac{Z_t(\omega) - Z_c}{Z_t(\omega) + Z_c} \qquad (A7)$$

where Z_c represents the parallel combination of upper and lower body R_cs.

The eight parameters that would ordinarily be needed to solve *Eqs. A6* and *A7* can be reduced to six by making use of data from the literature describing both the ratios of upper to lower body resistances and of the R_cs. Using data from Cox (9), we estimated an upper-to-lower body resistance ratio of 2.33 and a R_c ratio of 1.16. Thus, by specifying only six parameters, ω_c and T_d for both the upper and lower body tubes, R_{DC} for the total arterial system, and Z_c, *Eqs. A6* and *A7* could be solved easily.

We gratefully acknowledge the intellectual contribution to this work made by Drs. William C. Hunter, Bram Zuckerman, and David T. Yue. We also thank Dr. Edward L. Yellin for his enthusiastic support and outstanding editorial consultation during the final stages of preparing the manuscript.

J. Alexander, Jr., was supported by Medical Scientist Training Program Grant 5T32-GM-07309. Other support for this research was provided by National Heart, Lung, and Blood Institute Research Grant R01-HL-18912.

Address for reprint requests: K. Sagawa, Dept. of Biomedical Engineering, Rm. 223 Traylor Bldg., The Johns Hopkins Medical School, 720 Rutland Ave., Baltimore, MD 21205.

Received 28 June 1988; accepted in final form 20 April 1989.

REFERENCES

1. ABEL, F. L. Fourier analysis of left ventricular performance. *Circ. Res.* 28: 119–135, 1971.
2. ALEXANDER, J., JR., D. BURKHOFF, AND J. SCHIPKE. Effect of mean arterial pressure on systemic arterial input impedance (Abstract). *Circulation* 76: IV-543, 1987.
3. AVOLIO, A., AND M. F. O'ROURKE. Application of multibranched digital computer model to hemodynamic studies of the mammalian arterial system (Abstract). *Excerpta Med. Int. Congr. Ser.* 405: 2, 1976.
4. BARGAINER, J. D. Pulse wave velocity in the main pulmonary artery of the dog. *Circ. Res.* 20: 630–637, 1967.
5. BERGEL, J. D. The static elastic properties of the arterial wall. *J. Physiol. Lond.* 156: 445–457, 1961.
6. BURKHOFF, D., J. ALEXANDER, JR., AND J. SCHIPKE. Assessment of Windkessel as a model of aortic input impedance. *Am. J. Physiol.* 255 (*Heart Circ. Physiol.* 24): H742–H753, 1988.
7. COX, R. H. Determinants of systemic hydraulic power in unanesthetized dogs. *Am. J. Physiol.* 226: 579–587, 1974.
8. COX, R. H. Pressure dependence of the mechanical properties of

arteries in vivo. *Am. J. Physiol.* 229: 1371–1375, 1975.
9. COX, R. H., AND J. B. PACE. Pressure-flow relations in the vessels of the canine aortic arch. *Am. J. Physiol.* 228: 1–10, 1975.
10. LATSON, T. W., W. C. HUNTER, N. KATOH, AND K. SAGAWA. Effect of nitroglycerine on aortic impedance, diameter, and pulse wave velocity. *Circ. Res.* 62: 884–890, 1988.
11. LIU, Z., K. BRIN, AND F. C. P. YIN. Estimation of total arterial compliance: an improved method and evaluation of current methods. *Am. J. Physiol.* 251 (*Heart Circ. Physiol.* 20): H588–H600, 1986.
12. MARMARELIS, P. Z., AND V. Z. MARMARELIS. *Analysis of Physiologic Systems; the White-Noise Approach.* New York: Plenum, 1978.
13. MCDONALD, D. A. Regional pulse wave velocity in the arterial tree. *J. Appl. Physiol.* 24: 73–78, 1968.
14. MCDONALD, D. A. *Blood Flow in Arteries* (2nd ed.). London: Arnold, 1974.
15. MILNOR, W. R. Arterial impedance as ventricular afterload. *Circ. Res.* 36: 565–570, 1975.
16. MURGO, J. P., N. WESTERHOF, J. P. GIOLMA, AND S. A. ALTOBELLI. Aortic input impedance in normal man: relationship to pressure wave shape. *Circulation* 62: 105–116, 1980.
17. MURGO, J. P., N. WESTERHOF, J. P. GIOLMA, AND S. A. ALTOBELLI. Manipulation of ascending aortic pressure and flow wave reflections with the Valsalva maneuver: relationship to input impedance. *Circulation* 63: 122–132, 1981.
18. NOBEL, M. I. M. Left ventricular load, arterial impedance and their interrelationship. *Cardiovasc. Res.* 13: 183–198, 1979.
19. NOBEL, M. I. M., I. T. GABE, D. TRENCHARD, AND A. GUZ. Blood pressure and flow in the ascending aorta of conscious dogs. *Cardiovasc. Res.* 1: 9–20, 1967.
20. O'ROURKE, M. F. Pressure and flow waves in systemic arteries and the anatomical design of the arterial system. *J. Appl. Physiol.* 23: 139–149, 1967.
21. O'ROURKE, M. F. *Arterial Function in Health and Disease.* Edinburgh: Churchill Livingstone, 1982.
22. O'ROURKE, M. F., AND A. P. AVOLIO. Pulsatile flow and pressure in human systemic arteries: studies in man and in a multibranched model of the human systemic arterial tree. *Circ. Res.* 46: 363–372, 1980.
23. O'ROURKE, M. F., AND M. G. TAYLOR. Input impedance of the systemic circulation. *Circ. Res.* 20: 365–380, 1967.
24. PATEL, D. J., F. N. DEFREITAS, AND D. L. FRY. Hydraulic input impedance to the aorta and pulmonary artery in dogs. *J. Appl. Physiol.* 18: 134–140, 1963.
25. PEPINE, C. J., W. W. NICHOLS, AND C. R. CONTI. Aortic input impedance in heart failure. *Circulation* 58: 460–465, 1978.
26. SIPKEMA, P., AND N. WESTERHOF. Effective length of the arterial system. *Ann. Biomed. Eng.* 3: 296–307, 1975.
27. TAYLOR, M. G. Wave travel in arteries and the design of the cardiovascular system. In: *Pulsatile Blood Flow*, edited by E. O. Attinger. New York: McGraw, 1965, p. 343–372.
28. TAYLOR, M. G. Use of random excitation and spectral analysis in the study of frequency-dependent parameters of the cardiovascular system. *Circ. Res.* 18: 585–595, 1966.
29. TAYLOR, M. G. The input impedance of an assembly of randomly branching elastic tubes. *Biophys. J.* 6: 29–51, 1966.
30. WESTERHOF, N. *Analog Studies of Human Systemic Hemodynamics* (PhD thesis). Philadelphia, PA: Univ. of Pennsylvania, 1968.
31. WESTERHOF, N., F. BOSSMANN, C. J. DE VRIES, AND A. NOORDERGRAAF. Analog studies of the human systemic arterial tree. *J. Biomech.* 2: 121–143, 1969.
32. WESTERHOF, N., P. SIPKEMA, G. C. VAN DEN BOS, AND G. ELZINGA. Forward and backward waves in the arterial system. *Cardiovasc. Res.* 6: 648–656, 1972.